AAAS
Space: Science & Technology
Volume 2021, Article ID 7592858, 14 pages
https://doi.org/10.34133/2021/7592858

Space: Science & Technology
A SCIENCE PARTNER JOURNAL

Review Article

Applications of Vacuum Measurement Technology in China's Space Programs

Detian Li, Yongjun Wang, Huzhong Zhang, Zhenhua Xi, and Gang Li

Science and Technology on Vacuum Technology and Physics Laboratory, Lanzhou Institute of Physics, Lanzhou 730000, China

Correspondence should be addressed to Detian Li; lidetian@hotmail.com and Gang Li; ligangcasc510@163.com

Received 2 August 2020; Accepted 21 October 2020; Published 27 February 2021

The significance of vacuum measurement technology is increasingly prominent in China's thriving space industry. Lanzhou Institute of Physics (LIP) has been dedicated to the development of payloads and space-related vacuum technology for decades, and widely participated in China's space programs. In this paper, we present several payloads carried on satellites, spaceships, and space stations; the methodologies of which covered the fields of total and partial pressure measurement, vacuum and pressure leak detection, and standard gas inlet technology. Then, we introduce the corresponding calibration standards developed in LIP, which guaranteed the detection precision of these payloads. This review also provides some suggestions and expectations for the future development and application of vacuum measurement technology in space exploration.

1. Introduction

Vacuum is a ubiquitous existence in the universe. A spacecraft will experience a pressure range of more than ten orders of magnitude, including atmospheric pressure, low vacuum, high vacuum, ultrahigh vacuum (UHV), and extreme high vacuum (XHV), since launching from the Earth. In deep space, vacuum degree varies greatly, for example, the atmospheric pressure on Moon surface is about 10^{-8}-10^{-10} Pa, and on Mars is about 700 Pa, while interplanetary vacuum is as low as 10^{-10}-10^{-14} Pa. On-site measurement of vacuum degree in real time is one of the major tasks for space exploration: on the one hand, accurate acquisition of vacuum degree in spacecraft orbit space, interplanetary space, and planet surface is the most basic goal of space tasks; on the other hand, the measurement of leakage rate is of great significance to protect the life and health of astronauts in manned space missions. In order to get accurate measurement results, meters of all kinds must be calibrated with established vacuum metrology standards. Vacuum metrology has become an independent branch of metrology, covering measurement and calibration of total pressure, partial pressure, gas micro flow (leak rate), pressure leak, etc. [1]. Some important national metrology research institutions in the world have built branches dedicated to vacuum metrology research, such as the National Institute of Standards and Technology (NIST) of the United States, the Physikalisch-Technische Bundesanstalt (PTB) of Germany, and the National Physical Laboratory (NPL, which has given up its vacuum section in 2008) of the United Kingdom.

Lanzhou Institute of Physics (LIP) is one of the most important institutions devoted to vacuum technology in China. Since 1962, LIP has built a family of apparatuses covering all of the abovementioned vacuum metrology requirements [2], serving China's industry sectors such as national defense, aerospace, and civil industry. All the apparatuses developed in LIP are traced to the standards built in National Institute of Metrology (NIM) of China; besides, several intercomparisons have been implemented with PTB [3]. LIP is also committed to pushing forward the frontier of vacuum science. There are two mainstream basic methods for vacuum calibration around the world: static expansion method (SEM) and dynamic flow method (DFM). The advantages of the SEM standard device are simple structure and small measurement uncertainty, so most countries regard this kind of apparatuses as the primary standard for low vacuum metrology [4]. However, the lower limit of SEM method is limited to 10^{-5} Pa resulting from the outgassing of the calibration chamber. We proposed a novel approach based on the idea of selective pumping, with which the lower limit of the SEM standard was extended to 10^{-7} Pa [5, 6]. DFM is a widely recognized method for high vacuum calibration, based on

which LIP developed a standard with a lower limit of 10^{-7} Pa [7]. To extend the lower limit, a separated flow method was adopted with the combination of turbo molecular pump (TMP) and nonevaporable getter pump (NEGP) to obtain an ultimate pressure of 10^{-10} Pa [8]. This apparatus works at room temperature, so the heat effect produced by cryopumps commonly used in similar equipment can be eliminated and an improved combined standard uncertainty is obtained (3.5%). With the lower limit of constant conductance gas flowmeter extended to 10^{-12} Pa·m^3/s, the combined standard uncertainty is reduced to 0.94% ($k = 1$) [9].

In recent years, some important space missions have been launched in China, including manned space program, Moon exploration, and BeiDou navigation satellite system. In manned space program, leak detection is needed for the docking plane and cabin door to guarantee astronaut's life and space mission's success. In moon exploration, a lunar soil sealing equipment with very low leak rate is needed to get uncontaminated lunar soil back to the Earth. In BeiDou Navigation Satellite System, standard gases inlet method is indispensible to get suitable buffer gases in rubidium bubble for enhanced performance of the satellite-borne rubidium atomic clock, which is the most important payload of the system.

To meet the above requirements in space, some novel measurement instruments and calibration standards have been developed in LIP. In this review, typical works carried out in LIP and their applications in China's aerospace will be presented.

2. Total Pressure Measurement and Calibration

2.1. Total Pressure Measurement in Space Programs. In order to achieve in situ accurate measurement in Apollo mission, National Aeronautics and Space Administration (NASA) developed a cold cathode ionization gauge with a measurement range of 10^{-10}-10^{-6} Pa and a measurement uncertainty of 40%. On Apollo 12, 14, and 15 spacecraft, the vacuum gauge was carried to directly measure the vacuum on the lunar surface. Testing results verified that vacuum degree on lunar surface is between 10^{-8} Pa (sunrise) and 10^{-10} Pa (sunset), which is the only understanding of the lunar atmospheric pressure by human beings so far [10, 11]. In 2004, European Space Agency (ESA)'s Rosetta comet detector was equipped with a field emission cathode ionization gauge, effectively reducing the nominal power consumption to 0.72 W, achieving measuring range of 10^{-9}-10^{-2} Pa, and sensitivity of 0.05 Pa^{-1} (N_2). The detector arrived at comet Churyumov-Gerasimenko in 2014 and analyzed the static atmospheric pressure and dynamic pressure on its surface (equivalent to measuring the gas flow of comet), which were, respectively, used to study the gas dust dynamics characteristics of comets and satellite attitude control. At present, the only reported space ultrahigh vacuum gauge in China was carried on the "Shenzhou" series spacecraft [12]. The core sensor is a Bayard-Alpert ionization vacuum gauge; it can measure the pressure range of 10^{-7}-10^{-4} Pa. In orbit operation, the high-speed data transmission system on board will send the atmospheric pressure, temperature, and other data back to the ground, and the corresponding orbit and attitude data will be given by the spacecraft engineering system at the same time. After the ground synthesis processing, the space environment atmospheric density and its change status on the orbit height will be obtained.

Efforts have also been made for the measurement of total pressure in LIP. Since 2013, we have carried out theoretical and experimental research on carbon nanotube (CNT) cathode ionization gauge cooperated with Lanzhou University, Wenzhou University, and Bern University of Switzerland [13–22]. First, we established a three-dimensional physical model of CNT ionization gauge and used SIMION software to simulate the influence of electrode voltage, gate structure, and physical transmittance, etc. on sensitivity, based on which the structural and electrical parameters of the high sensitivity ionization gauge were determined [13]. Second, preparation process of CNTs with enhanced performance was developed: uniform and vertical multiwall CNTs were prepared by anodic alumina template method and deposition catalyst method to improve field emission performance [14, 15]; free distribution CNTs were directly grew and prepared by oxidation-reduction method to improve emission current density and stability [16, 17]. Third, a series of CNT cathode ionization gauges, such as Bayard-Alpert type, separation type, and spherical oscillator type, have been developed based on the abovementioned works [18–22] as shown in Figure 1. Among them, the separation-type CNT cathode ionization gauge has reached the best level reported at present. In the range of 10^{-9} Pa to 10^{-4} Pa, ion current received by collector has good linearity with pressure. Good long-term stability has also been observed: the fluctuation of 12 months for N_2 and Ar is 1.6% and 2.0%, respectively. Since 2017, we have set out the development of Micro-Electro-Mechanical System- (MEMS-) type capacitance diaphragm gauge (CDG). A theoretical model considering size effect was established to examine mechanical properties of microscale pressure-sensing film [23]; edge field effect was discussed and eliminated for capacitance [24]. Key technologies, such as the preparation of large wide-to-thickness ratio flat pressure sensing film and the development of nanogetter film [25], have been tackled. The principle prototype of MEMS-type capacitance diaphragm gauge has been developed [26], and preliminary tests have been carried out, as shown in Figure 2. The lower limit of measurement is 5 Pa.

2.2. Calibration of Total Pressure Gauges. NASA established a UHV/XHV calibration system based on molecular beam method for Apollo lunar exploration in the 1960s [27]. The system combined the molecular beam method, pressure attenuation method, and low-temperature pumping technology. It can calibrate the ultrahigh vacuum gauges between 10^{-11} Pa and 10^{-6} Pa, with calibration error less than 5%. Aiming at ground and space in situ calibration of the field emission cathode ionization gauge, ESA has developed the CASYMIR system, which can simulate the ultrasonic jet molecular beam and carry out ultrahigh vacuum calibration under the conditions of temperature environment [28]. The calibration device is composed of a heated vacuum system, a gas supply system, and a control system. The calibration range is 10^{-8}-10^{-3} Pa, and

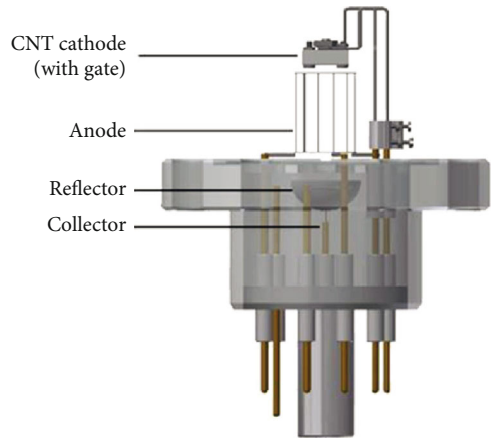

Figure 1: Setup of the CNT cathode ionization gauge [20].

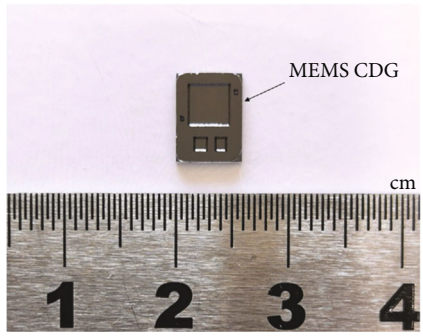

Figure 2: MEMS-type capacitance diaphragm gauge [26].

temperature range is 295-550 K. In order to accurately calibrate the space vacuum gauge carried by Shenzhou spacecraft, a calibration system has been developed based on dynamic flow conductance method [29]. The limit vacuum of calibration chamber is 2.7×10^{-7} Pa, and the calibration range is $1.3 \times 10^{-6} - 1.3 \times 10^{-2}$ Pa.

In 2008, in order to meet the needs of aerospace, high energy physics, surface science, microelectronic devices, and other fields for UHV precise calibration, we developed a new generation of static expansion vacuum standard [5] (Figure 3) based on the research of static expansion vacuum standard, with a measurement range of $4 \times 10^{-7} - 1 \times 10^{4}$ Pa and an expanded uncertainty of 2.2-0.3% ($k = 2$). Through tackling a series of key technologies, such as the extension of the lower calibration limit, the accurate measurement of the volume and volume ratio of the vacuum vessel, the detection of tiny leaks, the degassing of the vacuum material, and the measurement of the outgassing rate, the lower calibration limit of the device was extended two orders of magnitude down from the best level (10^{-5} Pa) of the reported similar standards worldwide and reached 10^{-7} Pa for the first time [5].

In view of the wide application value of extremely high vacuum measurement and calibration technology in space program, nuclear fusion, and high-energy particle accelerator, etc., a UHV/XHV vacuum standard was constructed in LIP based on the creatively proposed ideas of flow separation

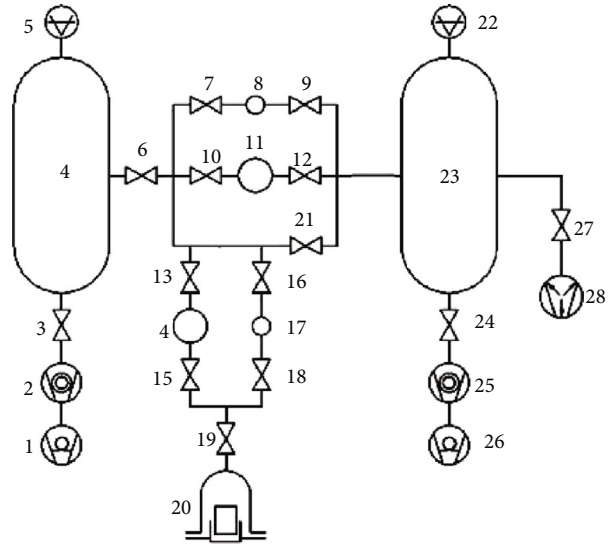

Figure 3: Static expansion vacuum standard with extended low-pressure range [5]. 1 and 26: rotary pumps; 2 and 25: TMP; 3, 6, 7, 9, 10, 12, 13, 15, 16, 18, 19, 21, 24, and 27: isolation valves; 4: left calibration chamber; 5 and 22: ionization gauges; 8 and 17: 0.1 l sampling vessels; 11 and 14: 1 l sampling vessels; 20: DPG8 and FRS5; 23: right calibration chamber; and 28: NEGP.

and selective pumping background extension [6–8] (Figure 4). The measurement range is 10^{-10}-10^{-1} Pa, and the expanded uncertainty is 7-0.9% ($k = 2$). In 2014, we drafted the calibration specification of very high vacuum ionization gauge based on flow separation method covering 5×10^{-10} -5×10^{-6} Pa [30]. Based on the progress of micro flow technology, the lower measurement limit of the constant conductance method gas micro flowmeter was extended to the order of 10^{-12} Pa · m^3/s [9], which was applied to the UHV/XHV vacuum standard, and the uncertainty component introduced by the flow separate ratio in the abovementioned method was reduced to 0.94%. In 2019, research results of the new type constant conductance element were introduced into the UHV/XHV vacuum standard [31]. With the expansion of the upper limit of molecular flow, the measurement uncertainty can be further reduced while obtaining the same level of gas micro flow in the constant conductance method gas micro flowmeter.

3. Manned Space Program

3.1. Development of the Port Quick Leak Detector. The docking plane and cabin door are the passageways through which the space station realizes personnel and material exchanges with spaceships; besides, personnel can implement spacewalk to carry out experiments and maintenance tasks. The seal quality of the docking plane and cabin door plays a decisive role to ensure the safety of astronauts and spacecraft instruments [32]. Ground leakage rate detection has a certain reference value, but due to frequent on-orbit opening and closing, reliable on-orbit quick monitoring device must be developed to grasp the sealing quality in real time.

To detect the leakages of docking plane and cabin door, a simple leak detection method was put forward according to

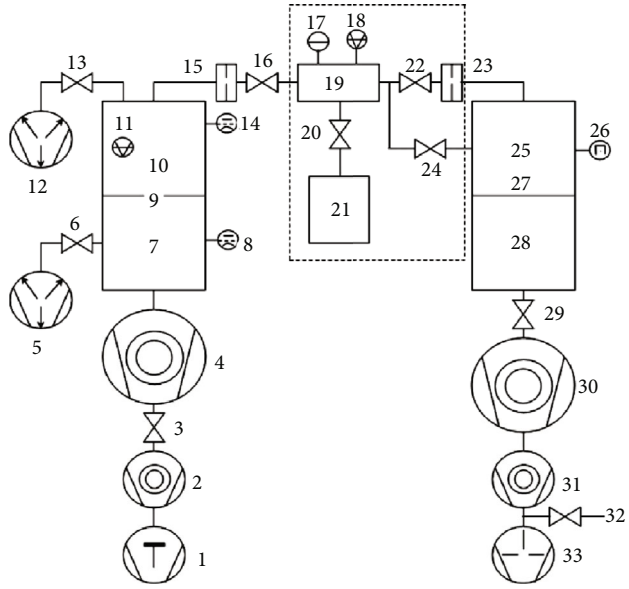

Figure 4: Vacuum calibration apparatus with pressure down to 10^{-10} Pa [8]. 1: dry pump; 2, 4, 30, and 31: TMP; 3, 6, 13, 16, 20, 22, 24, and 29: isolation valve; 5 and 12: NEGP; 7: XHV pumping chamber; 8 and 14: hot cathode ionization gauge; 9, 15, 23, and 27: orifice; 10: XHV calibration chamber; 11 and 18: spinning rotor gauge; 17: capacitance-diaphragm gauge; 19: separated flow chamber; 21: flowmeter; 25: UHV calibration chamber; 26: cold cathode ionization gauge; 28: UHV pumping chamber; 32: venting valve; and 33: rotary pump.

the sealing structure [33], as shown in Figure 5. A small vessel with a volume V of about 50 ml is formed between the two sealing rings of the cabin door. Fill the vessel with trace gas $p_0$and then monitor the inside pressure change $\Delta p = p_0 - p_t$ by detecting vessel pressure $p_t$after time Δt. The leakage rate Q can be expressed as follows:

$$Q = \frac{p_0 - p_t}{\Delta t} V. \tag{1}$$

This method has advantages of fast pressure change and high sensitivity; based on which, we developed an on-orbit device port quick leak detector (PQLD), as shown in Figure 6. The accurate measurement of small volume for complex structure is critical in leak detection, and hence, an in situ measurement method was used. The small volume was determined by gas static expansion method combined with a reference rod with a known volume of V_d, as shown in Figure 7. When the rod is out of the external vessel, we have the following:

$$p_1 V = p_2 \left(V + V' \right). \tag{2}$$

When the rod is inserted into the external vessel, we have the following:

$$p_3 V = p_4 \left(V + V' - V_d \right), \tag{3}$$

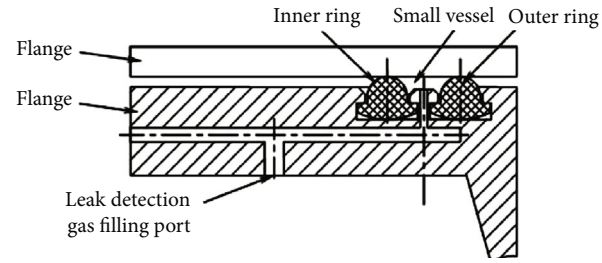

Figure 5: Schematic diagram of port leakage detection.

where p_1 and p_3 are the pressures inside the small vessel before expansion; p_2 and p_4 are the pressures after expansion. Then, we can get the volume of the small vessel V by Equation (2) and Equation (3)

$$V = \frac{1}{(p_1/p_2) - (p_3/p_4)} V_d. \tag{4}$$

The detector will automatically complete the work in space. Aiming at the task characteristics of the PQLD, the system design provides the function of data injection. According to the requirements of specific detection, the system can set the initial parameters through special ground inspection equipment whenever needed without occupying the remote control channel and telemetry channel; meanwhile, the detection results can be obtained within 8 min. A number of low-power design technologies have been adopted in the hardware and software design, which effectively reduces the power consumption of the system (the power consumption is 6.8 W, the total weight is 5 kg, and the volume is 7.9 dm^3).

3.2. Calibration Method of the PQLD. The calibration of the PQLD is essentially pressure leak calibration. There are three methods for the calibration of pressure leaks: constant volume-variational pressure method (CVVP), constant pressure-variational volume method (CPVV), and dynamic state compare method (DSCM) [34–36]. We have built both apparatuses based on CVVP and CPVV, which are competent for the calibration demands of the PQLD.

The CPVV calibration apparatus developed in LIP [37] is shown in Figure 8. When the gas from leak is introduced into variable chamber, the piston moves out to keep constant pressure. The leak rate Q can be calculated by measuring movement distance l of the piston and movement time t. The saw-tooth wave constant pressure principle is adopted [36]. The change of pressure with time is saw-tooth variation by controlling piston movement intermittently, which can ensure the initial pressure equal to the end pressure. The constant temperature water tank and piston seal with sleeve-type connector were proposed, which reduced the background leak rate caused by temperature fluctuation and dynamic sealing. The virtual flow induced by temperature fluctuation is controlled around 2.4×10^{-9} Pa · m^3/s. The background leak rate is about 6×10^{-10} Pa · m^3/s, which can be obtained when the piston moves in maximal and minimal velocity. The leak rate measurement was achieved automatically using

Figure 6: The on-orbit device port quick leak detector.

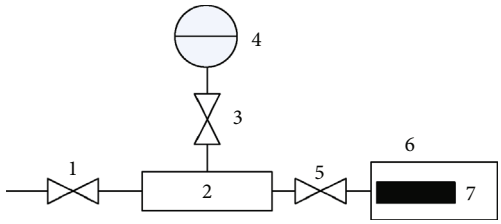

Figure 7: Method to determine the vessel's volume V. 1, 3, and 5: valves; 2: small vessel; 4: gas supply; 6: external vessel V'; and 7: reference volume rod V_d.

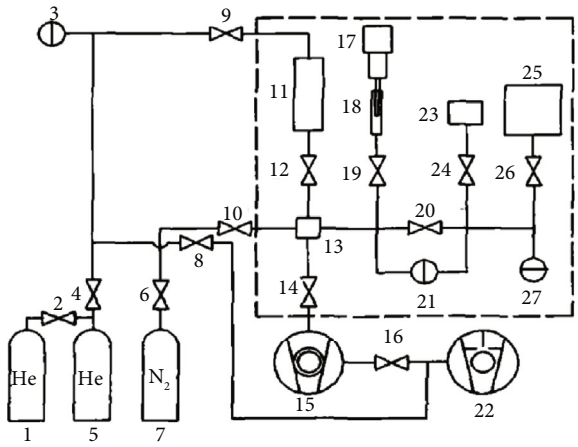

Figure 8: Schematic diagram of apparatus based on CPVV [37]. 1, 5, and 7: gas reservoir; 2, 4, 6, 8, 9, 10, 12, 19, 20, 24, and 26: valve; 3, 21, and 27: CDG; 11: pressure leak; 13: invariable chamber; 14: angle valve; 15: TMP; 16: electromagnetism valve; 17: servomotor; 18: variable chamber and piston; 22: rotary pump; and 23 and 25: standard chamber.

virtual instrument technique. The lower limit of measurement is as low as 10^{-7} Pa · m^3/s. The uncertainty of this apparatus is contributed by (1) the uncertainty of the pressure measurement; (2) the uncertainty of the piston volume measurement; (3) the uncertainty of time measurement; (4) the uncertainty of the temperature measurement; (5) temperature fluctuation; and (6) measurement of the standard volume. The combined standard uncertainty can be calculated to be 3.1%.

Recently, a new calibration apparatus based on direct comparison calibration method and pressure-rising method with a constant volume has been designed and constructed in LIP [38]. This apparatus is made up of the standard leak rate system, calibration system, temperature control system, gas supply, and pumping system, which is able to obtain accurate leak rate using the standard leak rate system, as shown in Figure 9. The system mainly works in the temperature control unit (red dashed rectangle), which enables leak rate calibration at temperature ranging from -50°C to 20°C. The calibration principle is indicated in Figure 10. The calibration apparatus 1 generates a standard leak rate that is injected into calibration chamber 5; meanwhile, the PQLD measures the standard leak rate by testing pressure changing in chamber 5. The correction factor of the PQLD can be calculated by the comparison between the measurement results and the standard leak rate given by the apparatus. The standard leak rate provided by the apparatus varies from 2.43×10^{-6} Pa to 2.25×10^{-2} Pa, covering the PQLD calibration demand of 10^{-4}-10^{-2} Pa. The correction factor is increased with temperature, indicating further correction should be carried out considering the influence of temperature. For different gases, the correction factor for N_2, Ar, and He is 1.07, 1.08, and 1.08, respectively, indicating gas species exert little effect on calibration results. The uncertainty of this apparatus is contributed by (1) the uncertainty of the standard leak rate; (2) leak detector reading; (3) total volume parameter of the leak detector and the apparatus; (4) temperature fluctuation; and (5) temperature homogeneity. The combined standard uncertainty can be calculated to be 4.7%.

4. Lunar Sample Sealing Equipment

The formation, evolution, and characterization of the Moon, and even the answer to the questions regarding the genesis of the universe may lie in the composition of lunar soil. It has been the main target to get lunar samples back to the Earth since the beginning of Moon exploration. In July 1969, Apollo 11 spacecraft of the United States realized the first manned landing on the Moon. Successively, Apollo 12, 14, 15, 16, and 17 and the former Soviet Moon 16, 20, and 24 carried out manned and unmanned lunar landing and sampling. A total of 382 kg of lunar samples and massive scientific data were obtained [39]. Chinese lunar exploration strategy pointed that lunar samples should be collected on the lunar surface and be returned to the Earth [40, 41]. In order to guarantee the accuracy of the ground analysis, lunar sample must be sealed in a special container, inside which the original lunar environment can be maintained. Due to the atmospheric pressure on the Moon is about 10^{-10} Pa, the sealing performance of the container must be considered to protect sample from pollution on the way back to the Earth atmosphere [42, 43].

4.1. Development of a Lunar Sample Container. To meet the requirement of lunar sample returning, a lunar sample container with sealing design has been developed in LIP [44, 45], as shown in Figure 11. The sealing scheme took a metal knife edge seal as primary seal and a rubber ring seal

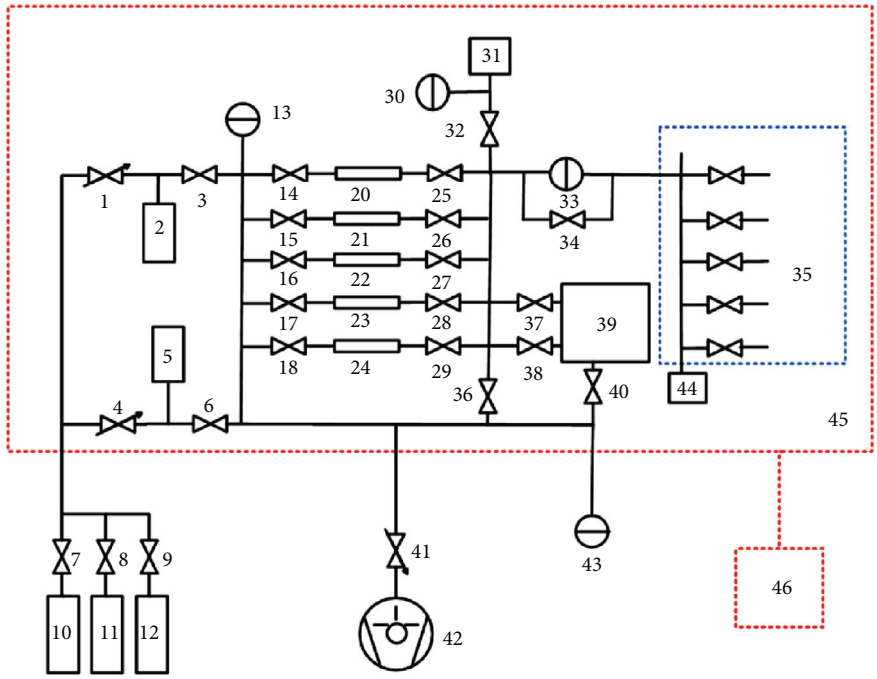

Figure 9: Schematic diagram of CVVP calibration apparatus [38]. 1, 4, and 41: adjusting valve; 3, 6, 8, 9, 14, 15, 16, 17, 18, 19, 25, 26, 27, 28, 29, 32, 34, 36, 37, 38, and 40: break valve; 2 and 5: ballast chamber; 10, 11, and 12: high-pressure cylinder; 13, 30, 33, and 43: capacitance diaphragm gauge (CDG); 20, 21,22, 23, and 24: pressure leak; 31: external container; 35: reference volume; 39: port quick leak detector; 42: vacuum pump; 44: constant temperature box; 45: small container; 46: temperature control unit.

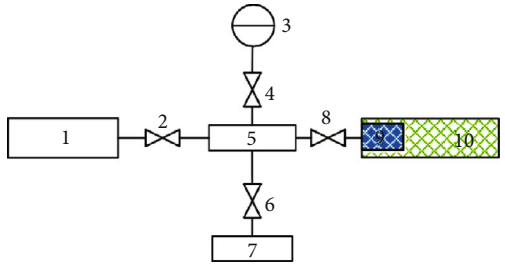

Figure 10: Calibration principle of CVVP calibration apparatus [38]. 1: standard leak rate system; 2, 4, 6, and 8: break valve; 3: measure instrument for gas pressure; 5: calibration chamber; 7: pumping system; 9: internal volume of leak detector; and 10: port quick leak detector.

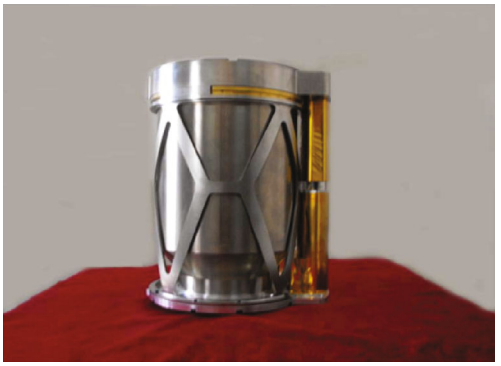

Figure 11: The lunar sample container developed in LIP.

as auxiliary seal. An indium-silver alloy volume and a rubber ring were mounted on the cover of the container, and the edge of the container was machined into a knife edge. The locking mechanism of the container provided a vertical downward pressure on the cover, making the knife edge blade into the alloy and the rubber ring be squeezed into the inner wall of the container, as shown in Figure 12. Thus, a radial seal was formed to insulate the sample from the external environment. Test results show that the leakage rate of the container is below 5×10^{-11} Pa · m^3/s [46], satisfying the requirement of lunar sample returning.

4.2. Vacuum Leak Rate Calibration. The leak rate to be calibrated is commonly compared to a known gas flow Q from the flowmeter using quadrupole mass spectrometers (QMS). A considerable error is witnessed caused by the nonlinearity of the QMS. Constant pressure gas flowmeter is often used to calibrate vacuum leaks, and its typical measurement range is from 10^{-3} Pa · m^3/s to 10^{-8} Pa · m^3/s. But for most vacuum leaks, such as the leak rate of the lunar sample container, their leak rates are commonly less than 10^{-8} Pa · m^3/s. Therefore, if the lower limit of gas flowmeter can be extended directly by a simple and feasible method, the uncertainty of nonlinearity produced by QMS can be avoided. To solve this problem, a constant conductance method gas flowmeter based on NEGP has been developed to accurately calibrate vacuum leaks with leak rates smaller than 10^{-8} Pa · m^3/s [9], as shown in Figure 13. The NEGP has two remarkable characteristics: (1) large pumping speed for active gases, especially for H_2 at ambient temperature,

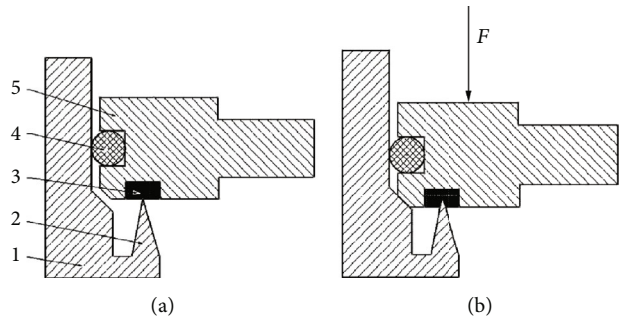

Figure 12: Schematic diagram of sealing scheme and sealing process: (a) before seal action and (b) after seal action [45]. 1: sample container; 2: knife edge; 3: indium silver alloy; 4: rubber ring; and 5: cover body.

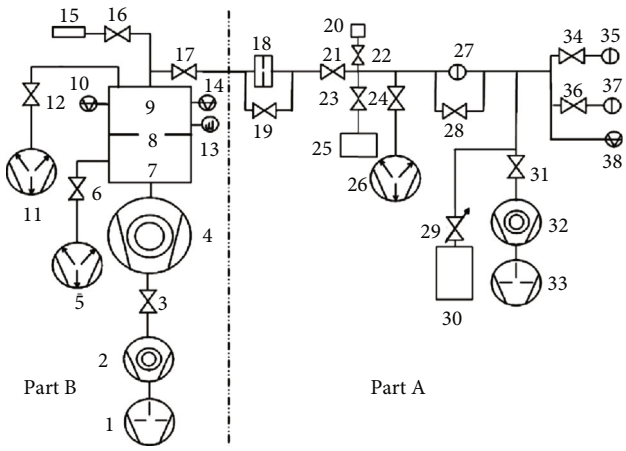

Figure 13: Scheme diagram of a very low gas flow measurement apparatus [9]. 1: dry pump; 2, 4, and 32: TMP; 3, 6, 16, 17, 19, 21, 22, 23, 24, 28, 31, 34, and 36: isolation valves; 5, 11, and 26: NEG pumps; 7: XHV pumping chamber; 8: orifice; 9: XHV calibration chamber; 10: calibrated ionization gauge; 13: quadrupole mass spectrometer; 14: ionization gauge; 15: calibrated leak; 18: small tube; 20: standard vessel; 25: ballast chamber; 27, 35, and 37: CDGs; 29: metering valve; 30: gas bottle; 33: rotary pump; and 38: SRG.

and (2) virtually zero pumping speed for inert gases. Because H_2 is the main residual gas in UHV/XHV systems, the introduction of NEGP will benefit the generation of UHV/XHV in the ballast chamber; besides, taking He as the test gas makes NEGP a choice for vacuum leak rate calibration. In molecular flow regime, the conductance value of a small tube is constant. The gas flow, Q, passing through small tube 18 can be determined by the following:

$$Q = \left(p - p'\right) C. \tag{5}$$

Practically, p is much larger than p':

$$Q = pC. \tag{6}$$

Normally, the vacuum leak rate is measured by the dynamic comparison method. However, when the leak rate is extremely low, the ion currents are difficult to be measured accurately. For the convenience of ion current measurement, static accumulation mode was used to increase ion current signals. The conductance of small tube 18 was measured in situ and real time by a constant volume method. The upstream side of the small tube 18 is connected to standard vessel 20; the volume of which is determined using volume expansion method. The downstream side of small tube 18 is connected to the XHV system (Part B). After He is injected into vessel 20, the pressure in the vessel, which will decrease with continuously pumped through small tube 18, will be monitored by CDG 27. Based on the gas flow conservation law, the conductance C of the small tube 18 can be obtained [9]. After reaching the ultimate pressure in ballast chamber 25, it will be isolated from the pump unit and filled with argon gas ranging from 2×10^{-3} Pa to 1×10^{2} Pa. Then, gas is passed through the small tube 18 with a conductance of the order of 10^{-9} m^3/s for argon at room temperature. The resulting gas flow can be calculated using Equation (6) to be 10^{-12} $Pa \cdot m^3/s$ to 10^{-7} $Pa \cdot m^3/s$. With the introduction of the NEGP, a low background pressure of less than 10^{-6} Pa is maintained stably in the ballast chamber 25 and pipes of the gas flowmeter. The uncertainty of outgassing is very small compared with the other components in the uncertainty budget. And the final combined standard uncertainty of the generated gas flow is 0.94% ($k = 1$).

5. Satellite-Borne Rubidium Atomic Clock

5.1. Key Technology in the Development of Rubidium Atomic Clock. Satellite navigation technique has penetrated into every aspect of daily life, national defense, industrial and agricultural production, etc. There are four mainstream systems worldwide: GPS of the USA, GLONASS of Russia, GALIEO of Europe, and BeiDou of China. As the core component aboard navigation satellites, the performance of rubidium atomic clocks dominates the positioning, navigation, and timing (PNT) accuracy directly [47, 48], which enables time measurement at the nanosecond level when signals travelling thousands of kilometers from space to the Earth.

In order to eliminate wall relaxation and Doppler broadening, buffer gas is injected into the ^{87}Rb absorption bubble [49, 50]. The use of mixtures of buffer gases, N_2 and Ar for instance, can reduce the temperature coefficient of the absorption bubble to a predetermined value [51]. Therefore, accurate matching and control technique for buffer gases are key techniques for performance enhancement of satellite-borne rubidium atomic clock [52, 53]. We have developed a high-precision rubidium atomic clock in LIP, which plays an irreplaceable and decisive role in the construction of China's BeiDou navigation system, as shown in Figure 14.

5.2. Standard Gas Inlet Technology. Due to the discrimination effect of the injection orifice and the pumping system on gases of different types and flow states, partial pressure of the introduced mixed gas will deviate from the standard mixed gas. Therefore, it is necessary to develop a proper

Figure 14: Physics package of rubidium atomic clocks developed in LIP.

standard gas inlet system to eliminate this deviation and to ensure the partial pressure constant in front of and behind the orifice [54].

The principle of the system developed in LIP is shown in Figure 15 [55]. It consists of pumping system, gas supply system, sample preparation system, sample injection system, and a calibration chamber. The basic idea of this system is to maintain molecular flow state during injection process; under this state, the gas composition will remain unchanged before and after injection [56]. Two gas inlet modes are optional: direct inlet mode and pressure decay mode. The former one applies to cases of standard gas pressure ranging from 10^2 to 10^{-1} Pa, making inequality hold [57]:

$$\bar{p} \times D \leq 2, \tag{7}$$

where $D = 0.02$ mm is the diameter of the orifice; $\bar{p} = (p_1 + p_2)/2$, where p_1 and p_2 are the pressures of the inlet and outlet, respectively. Due to p_1 is much larger than p_2, $p_1 \approx 2\bar{p}$. Thus, the upper limit of p_1 is 10^2 Pa. As for the pressure decay mode, it is capable of high-pressure standard gas of 10^2-10^5 Pa. First, high-pressure gas is injected into the 1 ml small volume 17; then, it is expanded into the 1 l sample inlet chamber 19 statically. After this procedure, the standard gas pressure will be reduced by 4 orders of magnitude, namely, 10^5 Pa will be abated to 10 Pa, and the molecular flow state holds for the system.

Performance tests have been carried out afterward [55]. The sample inlet chamber background pressure can be pumped as low as 10^{-6} Pa and raised to 9.8×10^{-3} Pa after 30 min, which meets the requirements considering the lower inlet limit of 10^{-1} Pa. For mixture of N_2 (33.1%), He (33.8%), and Ar (33.1%) from 10^5 Pa to 10^{-1} Pa, high consistency of relative sensitivity was observed: the relative standard deviation (RSD) of Ar versus N_2, He versus N_2, and He versus Ar is 2.15%, 3.66%, and 4.14%, respectively. The pressure ratio between the three gases remains basically unchanged under different inlet pressures, indicating the inlet pressure exerts limited influence on gas components. Repeatability tests with 3.0×10^2 Pa N_2, He, and Ar showed that the RSD of 6 tests is smaller than 0.1%. Under different mixed ratios of N_2 and Ar, the RSD of relative sensitivity is less than 1%, indicating excellent consistency. The good repeatability and consistency verified that the mixed gas composition has not been altered using the developed standard gas inlet system. The uncertainty of this system is contributed by (1) the uncertainty of the CDG; (2) the long-term instability of the CDG; (3) the uncertainty of the purity of a single gas; (4) outgassing of the sample preparation chamber; and (5) backflow of the sample preparation chamber. According to the above analysis, the uncertainty for 2—component standard gas—is calculated to be 2.2%, while 2.6% is for 3—component standard gas.

Thanks to the developed standard gas inlet system, accurate matching of buffer gases N_2 and Ar has been accomplished in the ^{87}Rb absorption bubble of the BeiDou satellite-borne rubidium atomic clock. The performance of the rubidium atomic clock has reached international advanced level, which has made an important contribution to the networking of BeiDou satellite navigation system.

6. Space Mass Spectrometer

Since the first flying of two double-focusing magnetic spectrometers on the Earth's upper atmosphere carried on Explorer XVII [58], mass spectrometry has become an indispensable payload in space explorations [59]. In order to meet the demands of space detection task, research on miniaturization of mass spectrometers, such as miniaturized magnetic sector, time of flight, quadrupole mass filter, and ion trap, have made significant progress recently [60–63]. This progress makes it possible to measure the concentrations of neutral-particle constituents of planets' atmosphere, monitor air quality on manned spacecrafts [64, 65], carry out isotopic analysis on asteroids to explore the origin of the universe [66], and search for evidence of life in space [67].

6.1. Development of a Miniature Magnetic Sector MS. Aiming at space exploration, we have developed a series of mass spectrometers, including TOF MS [68–70], ion trap MS [71–73], and magnetic sector MS (MMS) [74–76], among which a miniature MMS has been constructed and launched to 499 km Earth's orbit along with an experiment satellite in 2012 [76]. Compared with other mass spectrometers, MMS's advantages lie in simplicity, stability, high mass resolution and mass rejection ratio, and superior abundance sensitivity, making it a selection for atmospheric composition analysis and isotopic analysis [77]. This MMS, as shown in Figure 16, contains three parts: physical part, electronic control part, and high-voltage power supply part. The ion source has a Nier-type structure, with the focusing magnet of which the electron trajectory will be prolonged to enhance ionization probability. The analyzer is a 90° magnetic sector field with double channels: one is for mass range of 1~12 amu and the other one is for 6~90 amu. An electron multiplier with high negative potential is adopted to collect ions through the analyzer. The technical indices of this MMS are shown in Table 1.

This MMS has successfully detected the atmosphere compositions of the satellite orbit and gas emitted from the satellite, including O, He, $^{12}CO_2$, $^{13}CO_2$, H_2, N_2, O_2, and H_2O [76]. Figures 17 and 18 demonstrate typical mass spectra obtained on the 499 km orbit, which are consistent with that obtained by NASA's quadrupole mass spectrometer [78]. Isotope of $^{12}CO_2$ and $^{13}CO_2$ was captured in the spectrum, noting that the ratio of isotope deviates from the results

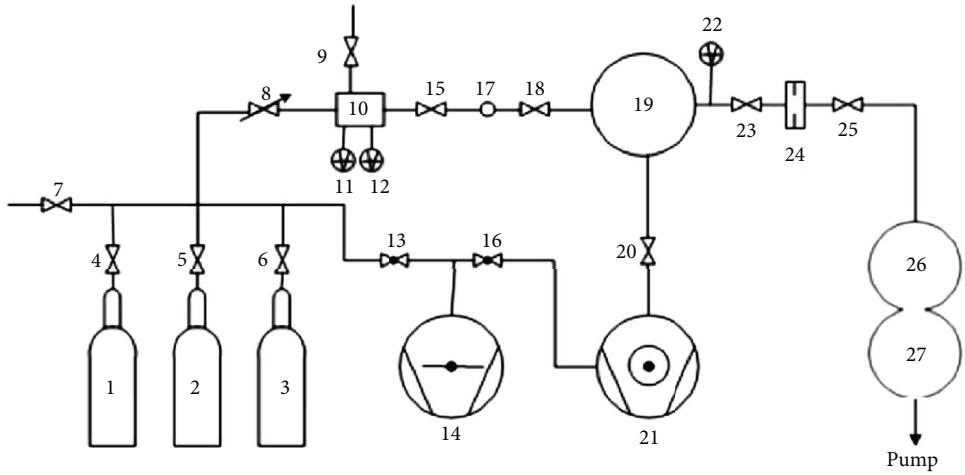

Figure 15: Schematic diagram of the standard gases inlet system [55]. 1, 2, and 3: high-pressure cylinder; 4, 5, and 6: break valve; 7, 9, 15, 18, 23, and 25: ball valve; 8: needle valve; 10: sampling chamber; 11 and 12: CDG; 13 and 16: isolation valve; 14: rotary pump; 17: small volume; 19: sample preparation chamber; 20: angle valve; 21: TMP; 22: ionization gauge; 24: orifice; 26: upper ball chamber; and 27: lower ball chamber.

Figure 16: Miniature magnetic sector mass spectrometer developed in LIP [76].

Table 1: Features and performance [76].

Mass analyzer	Magnetic sector field
Ion source	Nier-type ion source
Dimensions (mm^3)	$170 \times 165 \times 170$
Mass (kg)	4.5
Operating power (W)	18
Mass range (amu)	1-90
Resolution (amu)	<1
Sensitivity ($A \cdot Pa^{-1}$)	7.7×10^{-5}

obtained on the ground due to special space environment. The richest element on-orbit is O, and subsequently, N_2, O_2, H_2, CO, and CO_2. The content of H_2O is decreased with time, indicating that the detected H_2O is mainly from the satellite's adsorption on the Earth. Besides, He was also found in our work, which is closely related with solar wind and earthquake.

6.2. Partial Pressure Standard. In many circumstances, partial pressure of a specific component in a system is more attractive than the total pressure, which is usually measured by MSs. In order to transform the output of MSs into relative or absolute pressure, the MSs must be calibrated. In 1972, the American Vacuum Society published the calibration standard of partial pressure AVS standard 2.3-1972, in which the performance indices, working conditions, calibration system, and calibration method were described in detail. In 1993, a new standard was issued to replace the standard issued in 1972 [79]. In July 1987, mass spectrometry was listed as a legal metrological instrument in China, so it is urgent to study the partial pressure calibration technology and establish partial pressure calibration standards.

During the Ninth Five Year Plan (1996-2000), a partial pressure standard with calibrationable partial pressure ranging from 10^{-6} Pa to 10^{-1} Pa has been constructed in LIP [80], which is applied to the calibration of the abovementioned MMS. The standard, as shown in Figure 19, consists of gas supply system, gas introduction system, calibration room, and exhaust system. There are two calibration modes, corresponding to certain partial pressure ranges. For partial pressure from 10^{-4} Pa to 10^{-1} Pa, a magnetic levitation rotor gauge 15 connected to the calibration chamber 14 is used as reference standard to measure the partial pressure directly. Under the molecular flow state, rotor speed attenuation caused by collision of each gas component is independent due to there is no collision between gas molecules. Therefore, the total rotor speed attenuation is a linear superposition of the attenuations caused by all gas components. The partial pressure of each gas component can be obtained by calibrating the

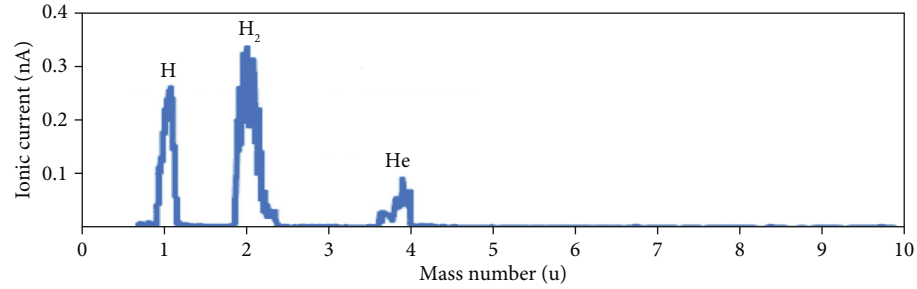

Figure 17: The typical mass spectra obtained from small channel [76].

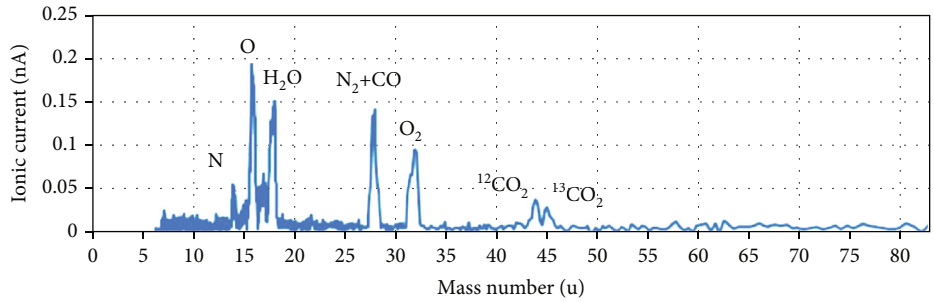

Figure 18: The typical mass spectra obtained from large channel [76].

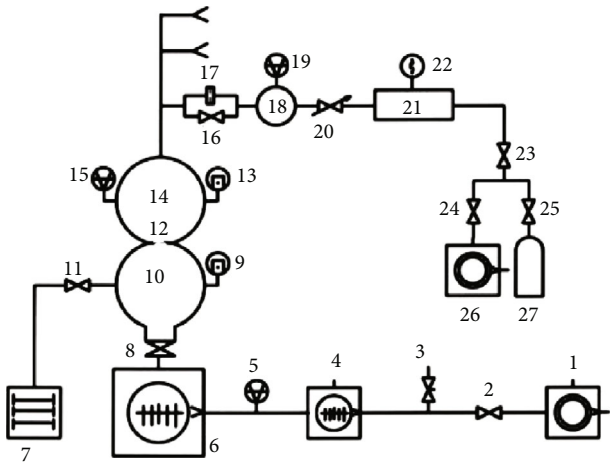

Figure 19: Schematic diagram of the MMS calibration system [80]. 1 and 26: dry pump; 2, 11, 16, 23, and 24: isolation valves; 3: vent valve; 4 and 6: TMP; 5: middle vacuum gauge; 7: NEG pump; 8: ultrahigh vacuum gate valve; 9 and 13: ultrahigh vacuum cold gauges; 10: pumping chamber; 12 and 17: orifices; 14: calibration chamber; 15 and 19: magnetic suspension rotor gauges; 18: upstream chamber; 20 and 25: metering valves; 21: pressure-stabilizing chamber; 22: Pirani gauge; and 27: gas bottle.

relative speed attenuation caused by each component. For partial pressure from 10^{-6} Pa to 10^{-4} Pa, pressure decay method is adopted using the upstream chamber 18. Close UHV angle valve 16 and adjust the pressure in the ballast chamber 21 to keep the pressure in chamber 18 to be 10^{-1} Pa to 10^{-4} Pa. Partial pressure in calibration chamber 14 can be obtained through the testing results of magnetic levitation rotor gauge 19. The uncertainty of the standard is less than 4.2% for pressure range of 10^{-4} Pa to 10^{-1} Pa, and 4.2% for pressure range of 10^{-6} Pa to 10^{-4} Pa. With the CF35 connectors and CF63 standard flanges on the calibration chamber, the magnetic spinning rotor gauge, cold gauge, and the calibrated mass spectrometer can be installed in the equatorial plane. With this standard, the MMS was calibrated to obtain its performance indices, such as peak position, sensitivity, and mass range [76].

Partial pressure measurements in UHV and XHV are gaining in importance in space programs. For example, on-site measurement of the Moon surface requires instrument with lower limit of 10^{-10} Pa. In order to cover the partial pressure calibration range of UHV and XHV, a new partial pressure standard, with the so-called "dynamic expansion method based on static expansion vacuum standard injection" mode, has been developed in LIP [81]. Figure 20 shows the scheme of the standard. It consists of a gas admission system, a static expansion system, and a dynamic expansion system. The principle is that a high-purity gas is firstly expanded from sampling chamber 7 into expansion chambers 18 and 20; then, the gas is expanded repeatedly between chambers 18 and 20 by pumping of chamber 20 in between; finally, the gas is introduced from chamber 20 into calibration chamber 32 to calibrate the mass spectrometer in a molecular flow state. The uncertainty of this system is mainly contributed by pressure measurement, expansion ratio, conductance calculation, conductance measurement, temperature fluctuation, fit function of conductance, and outgassing of expansion chamber, which is calculated to be 2.8-5.0% for N_2.

With the two partial pressure standards, partial pressure ranging from 10^{-10} Pa to 10^{-1} Pa has been covered, making LIP be capable of full-scale MS calibration. The performances of developed TOF MS, ion trap mass, and the MMS have

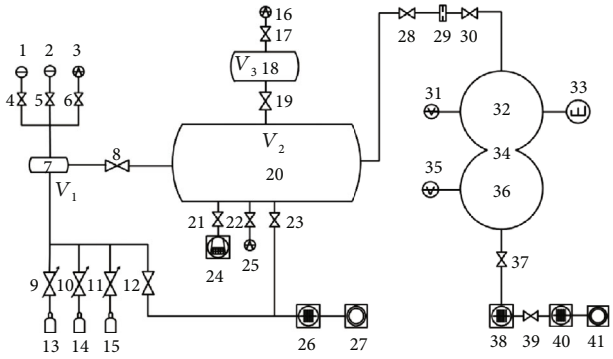

Figure 20: Schematic diagram of the UHV and XHV partial pressure calibration system [81]. 1 and 2: capacitance diaphragm gauges; 3, 16, and 25: combined gauges; 4, 5, 6, 8, 12, 17, 19, 21, 22, 23, 28, 30, 37, and 39: isolation valves; 7: sampling chamber; 9, 10, and 11: adjustable valves; 13, 14, and 15: gas bottles; 18 and 20: expansion chambers; 24: ion pump; 26, 38, and 40: TMP; 27 and 41: dry pump; 29 and 34: conductance element; 31 and 35: extractor gauges; 32: calibration chamber; 33: quadrupole mass spectrometer; and 36: pumping chamber.

been evaluated, verifying the significance of the two standards in China's space program.

7. Conclusion and Expectation

Space industry, with most of its components operating in vacuum environment, is highly linked to vacuum measurement technology. With the thorough implementation of China's deep space exploration, it is urgent to develop various scientific and engineering payloads to achieve all kinds of objectives. Atmospheric pressure of extraterrestrial bodies, such as planets, comets, and asteroids, is one of the most important and fundamental parameters, which can be measured by vacuum gauges. Considering the sharp pressure variation on different celestial bodies, it is necessary to select vacuum gauges suitable for certain pressure ranges. At present, Mars is one of the hot spots of space exploration in the world. Because the atmospheric pressure on Mars is hundreds of Pascal, MEMS-type capacitance diaphragm gauge may be the optimal choice to monitor pressure change on Mars for limited dimensions and energy consumption. In order to get precise and detailed analysis of the atmospheric and material composition, MSs are powerful tools to tackle this problem. MSs are classified according to mass analyzers, including magnetic sector, quadrupole, ion trap, and time of flight (TOF). The four types of MSs are suitable for different applications, for example, magnetic sector MS is an option to detect isotopes for high mass resolution capability, while the preference for comet volatile ingredients detection is TOF MS due to its rapid response ability. Ion propulsion system has recently been revealed and is a will-be-widely-used propulsion method in deep space exploration for fuel saving [82]. It is the key to generate a flat and tunable ion beam for the ion thruster to get stable thrust; the solution of which may lie in the reasonable design of gas inlet system. These are some of the typical payloads that LIP is working on. Due to the limitations in dimension and energy consumption demanded by space tasks, miniaturization is a major job to be done. In the past, the main idea was to optimize the payloads' structure at the expense of performance. With the continuous emergence of new technology and new materials, the situation has changed. MEMS is a technique with which sensors and electronic control systems can be made into microminiaturization. Both vacuum gauges and MSs can be fabricated using MEMS technique to achieve significant size reduction [26, 83]. Field emission is a brand new way to make low-energy consumption cathodes, which is the key component for a number of payloads. The ion trap MS of the Rosetta mission adopted nanotips etched on a silicon wafer as the field effect-based cathode [84]. The other approach to achieve field emission is via carbon nanotubes (CNTs) [85]. A series of CNT cathodes for vacuum gauges [20] and MSs [86] have been developed in LIP, with energy consumption dropping to the order of milliwatts. The emergence of miniaturized payloads based on new techniques such as MEMS and CNT is a game changer for space industry, making it possible for cost reduction, efficiency improvement, and the thriving micro/nanosatellites.

Compared with vacuum measurement carried out in laboratory, there are essential differences in cosmic vacuum measurement. The molecule movement state in cosmic environment is different from that in artificial vacuum containers. Ground vacuum measurement is to characterize the random moving, isotropic, and uniform gas molecular density in a limited container. In this case, the ideal gas equation of state, Maxwell's velocity distribution, cosine law, etc. can be in good agreement with the reality. In cosmic vacuum measurement, the object of measurement is the density of gas molecules in infinite space. In this case, the above theoretical models are no longer applicable. In the nonequilibrium state, the physical meaning of pressure and the measurement of vacuum degree are complex, so it is necessary to use new theory and method to carry out the research of cosmic vacuum measurement technology. It is an important tendency to replace the SI unit of pressure (Pascal) with quantum-based constant [87–89] and to build quantum-based primary standards. These new standards may enable zero-chain SI traceability, fast response, high accuracy, and unrestricted circumstance, which will fill the gap between ground and cosmic vacuum measurement. We have carried out preliminary studies on quantum-based primary standards, including refractive index method, absorption method, and cold atom method [90–92]. Knowing that we are still too far from "zero-chain traceability" in vacuum metrology and the question of traceability and comparison will remain in top interest for long, but it is worth pointing out that the quantum-based technology will be the key direction and inevitable trend of the development of vacuum metrology in the future.

Conflicts of Interest

The authors declare no conflict of interest.

Acknowledgments

The authors would like to acknowledge the support of the National Natural Science Foundation of China (Grant No. 61627805).

References

[1] L. Detian, *New Technology of Vacuum Metrology*, China Machine Press, 2013, Chinese.

[2] L. Detian, C. Xu, H. Yu, Z. Dixin, F. Weinan, and C. Liangzhen, *Developments of vacuum metrology in China*, Vacuum and Cryogenics, Chinese, 2004.

[3] L. Wangkui, L. Qiang, L. Zhenhai, G. Messer, and G. Grosse, "Intercomparison of vacuum standards between LIP and PTB," *Vacuum*, vol. 43, no. 11, pp. 1091-1092, 1992.

[4] A. Berman, "Vacuum gauge calibration by the static method," *Vacuum*, vol. 29, no. 11-12, pp. 417–425, 1979.

[5] D. Li, G. Zhao, M. Guo, J. Xu, and Y. Cheng, "Static expansion vacuum standard with extended low pressure range," *Mapan*, vol. 24, no. 2, pp. 95–100, 2009.

[6] L. Detian and C. Yongjun, "Applications of non evaporable getter pump in vacuum metrology," *Vacuum*, vol. 85, no. 7, pp. 739–743, 2011.

[7] Z. DX, L. DT, Y. Feng et al., "Vacuum calibration system by means of dynamic flow conductance," *Vacuum*, vol. 3, pp. 32–36, 2005.

[8] D. Li, M. Guo, Y. Cheng, Y. Feng, and D. Zhang, "Vacuum-calibration apparatus with pressure down to 10-10 Pa," *Journal of Vacuum Science & Technology A: Vacuum, Surfaces, and Films*, vol. 28, no. 5, pp. 1099–1104, 2010.

[9] L. Detian, C. Yongjun, F. Yan, X. Zhenhua, and Z. Lan, "Very low gas flow measurements for UHV/XHV and leak calibration," *Metrologia*, vol. 50, no. 1, pp. 15–19, 2013.

[10] P. A. Redhead, "History of ultrahigh vacuum pressure measurements," *Journal of Vacuum Science & Technology A: Vacuum, Surfaces, and Films*, vol. 12, no. 4, pp. 904–914, 1994.

[11] F. S. Johnson, J. M. Carroll, and D. E. Evans, "Lunar atmosphere measurements," *Proc Lunar Sci Conf*, vol. 3, pp. 2231–2242, 1972.

[12] Q. Guotai, ""SZ-3" atmospheric compositions detector measurement result-abnormal change of the upper atmosphere composition during geomagnetic activity disturbance on April 2002," *Chinese Journal of Space Science*, vol. 24, 2004.

[13] H. Z. Zhang, D. T. Li, C. K. Dong, Y. J. Cheng, and Y. H. Xiao, "Numerical simulation of electrode potential influence on the performance of ionization gauge with carbon nanotubes cathode," *Acta Physica Sinica*, vol. 62, no. 11, p. 110703, 2013.

[14] D. T. Li, Y. Cheng, M. Cai, J. L. Yao, and P. Chang, "Uniform arrays of carbon nanotubes applied in the field emission devices," *Science China Physics, Mechanics and Astronomy*, vol. 56, no. 11, pp. 2081–2084, 2013.

[15] D. Li, Y. Cheng, Y. Wang, H. Zhang, C. Dong, and D. Li, "Improved field emission properties of carbon nanotubes grown on stainless steel substrate and its application in ionization gauge," *Applied Surface Science*, vol. 365, pp. 10–18, 2016.

[16] Y. Wang, D. Li, W. Sun et al., "Synthesis and field electron emission properties of multi-walled carbon nanotube films directly grown on catalytic stainless steel substrate," *Vacuum*, vol. 149, pp. 195–199, 2018.

[17] J. Zhang, D. Li, Y. Zhao, Y. Cheng, and C. Dong, "Wide-range vacuum measurements from MWNT field emitters grown directly on stainless steel substrates," *Nanoscale Research Letters*, vol. 11, no. 1, p. ???, 2016.

[18] D. Li, Y. Cheng, Y. Wang et al., "Metrological properties of an ionization gauge with carbon nanotube cathode in different gases," *Vacuum*, vol. 125, pp. 222–226, 2016.

[19] D. Li, Y. Cheng, H. Zhang, Y. Wang, J. Sun, and M. Dong, "Investigation of an extractor gauge modified by carbon nanotubes emitter grown on stainless steel substrate," *Vacuum*, vol. 123, pp. 69–75, 2016.

[20] H. Zhang, Y. Cheng, J. Sun et al., "An ionization gauge for ultrahigh vacuum measurement based on a carbon nanotube cathode," *Review of Scientific Instruments*, vol. 88, no. 10, p. 105107, 2017.

[21] J. Sun, D. Li, Y. Cheng et al., "Development of an CNT field emission UHV ionization gauge with customized electronics," *AIP Advances*, vol. 8, no. 10, article 105020, 2018.

[22] H. Zhang, D. Li, P. Wurz et al., "Residual gas adsorption and desorption in the field emission of titanium-coated carbon nanotubes," *materials*, vol. 12, no. 18, p. 2937, 2019.

[23] G. Li, D. Li, Y. Cheng, W. Sun, X. Han, and C. Wang, "Design of pressure-sensing diaphragm for MEMS capacitance diaphragm gauge considering size effect," *AIP Advances*, vol. 8, no. 3, p. 035120, 2018.

[24] X. Han, D. Li, Y. Cheng, G. Li, and C. Wang, "Analysis on edge effect of MEMS capacitance diaphragm gauge with square pressure-sensing diaphragm," *Microsystem Technologies*, vol. 25, no. 7, pp. 2907–2914, 2019.

[25] C. Zhou, D. Li, H. Zhou, X. Liu, and Z. Ma, "Influence of the sputtering glancing angle on the microstructure and adsorption characteristics of Zr-Co-RE getter films," *Materials Research Express*, vol. 7, no. 3, p. 036402, 2020.

[26] X. Han, M. Xu, G. Li, H. Yan, Y. Feng, and D. Li, "Design and experiment of a touch mode MEMS capacitance vacuum gauge with square diaphragm," *Sensors and Actuators A: Physical*, vol. 313, p. 112154, 2020.

[27] P. Fowler and F. J. Brock, "Accurate, wide range ultrahigh-vacuum calibration system," *Journal of Vacuum Science and Technology*, vol. 7, no. 5, pp. 507–516, 1970.

[28] K. Altwegg, S. Graf, and E. Kopp, *A cometary neutral gas simulator for gas dynamic sensor and mass spectrometer calibration*, Egs-agu-eug Joint Assembly, 2003.

[29] S. Lilin, Q. Guotai, L. Xianwen, and L. Hong, "Ground calibration system for "SZ-3" atmospheric density detector and atmospheric composition detector," in *Conference of Special Committee on Space Exploration of Chinese Society of Space Research*, Chizhou, Anhui, China, 2002.

[30] *JJF 47-2014. Calibration specification for extreme high vacuum ionization gauge in the pressure range 5×10-10 Pa~5×10-6 Pa with separated-flow method*, SASTIND, 2014.

[31] Z. Xi, Y. Cheng, H. Zhang, Y. Li, and D. Li, "Uncertainty analysis of the LIP vacuum standard for XHV range," *Vacuum*, vol. 163, no. 5, pp. 275–281, 2019.

[32] S. B. Khan and J. R. Sanmartin, "Survival probability of round and tape tethers against debris impact," *Journal of Spacecraft and Rockets*, vol. 50, no. 3, pp. 603–608, 2013.

[33] C. Zhihe, C. Jun, Y. Xiaolin, Z. Xiaoyi, Q. Xin, and D. Yipeng, "Reliability and evaluating methods of port quick leak detector

for manned spacecraft," *Chinese Space Science and Technology*, vol. 3, p. 57, 2012.

[34] U. Wälchli, A. L. Stöckli, F. Rapp, M. A. Bösch, and A. Schmid, "Fundamental leak calibration system for gas leaks with a defined pressure difference over the leak element," *Journal of Vacuum Science and Technology*, vol. 14, no. 3, pp. 1247–1251, 1996.

[35] ASTM E908-98, "Standard practice for calibrating gaseous reference leaks," *American Society for Testing and Materials*, vol. 2012, 2012.

[36] K. Jousten and U. Becker, "A primary standard for the calibration of sniffer test leak devices," *Metrologia*, vol. 46, no. 5, pp. 560–568, 2009.

[37] F. Yan and Z. Dixin, "Design of pressure leak calibrator in constant pressure mode," *Chinese Journal of Vacuum Science and Technology*, vol. 5, pp. 442–445, 2007, (in Chinese).

[38] L. Zhao, Y. Cheng, W. Sun et al., "A new calibration apparatus of port quick leak detector for spacecraft," *MAPAN*, vol. 33, no. 2, pp. 91–97, 2018.

[39] J. Allton, *Lunar Samples: Apollo Collection Tools, Curation Handling, Surveyor III and Soviet Luna Samples*, APOLLO MISSION, 2009.

[40] O. Ziyuan, "Scientific objectives of Chinese lunar exploration project and development strategy," *Advances in Earth Science*, vol. 19, no. 3, pp. 351–358, 2004, (in Chinese).

[41] Y. Zheng, Z. Ouyang, C. Li, J. Liu, and Y. Zou, "China's Lunar Exploration Program: Present and future," *Planetary and Space Science*, vol. 56, no. 7, pp. 881–886, 2008.

[42] J. H. Allton, "Catalog of Apollo lunar surface geological sampling tools and containers," in *Tech. Rep. Contract NAS 9-17900*, Johnson Space Center, Texas, USA, 1986.

[43] F. D. Mundt, J. M. Schreyer, and W. E. Wampler, *Apollo Lunar sample return container–summary report*APOLLO MISSION.

[44] Y. Z. Du Yonggang, F. Zhaohui, J. Ming, and L. Haolin, "Feasibility study of the technology of automatic encapsulation for lunar sample," *Spacecraft Environment Engineering*, vol. 27, no. 5, pp. 566–569, 2010, (in Chinese).

[45] J. Ming, S. Liang, and M. Yang, "Seal design and test verification of lunar sample container," *IOP Conference Series Materials Science and Engineering*, vol. 439, article 042025, 2018.

[46] F. Zhaohui, M. Xu, and D. Yonggang, "Novel ultra high vacuum sealing technique with soft metal knife edge for space crafts," *Chinese Journal of Vacuum Science & Technology*, vol. 34, no. 3, pp. 221–224, 2014, (in Chinese).

[47] N. D. Bhaskar, J. White, L. A. Mallette, M. C. TA, and J. Hardy, "A historical review of atomic frequency standards used in space systems," in *International Frequency Control Symposium*, pp. 24–32, Honolulu, HI, USA, USA, June 1996.

[48] J. C. Camparo, "The rubidium atomic clock and basic research," *Physics Today*, vol. 60, no. 11, pp. 33–39, 2007.

[49] R. H. Dicke, "The effect of collisions upon the Doppler width of spectral lines," *Physical Review*, vol. 89, no. 2, pp. 472-473, 1953.

[50] H. G. Dehmelt, "Slow spin relaxation of optically polarized sodium atoms," *Physical Review*, vol. 105, no. 5, pp. 1487–1489, 1957.

[51] J. Vanier, R. Kunski, N. Cyr, J. Y. Savard, and M. Têtu, "On hyperfine frequency shifts caused by buffer gases: application to the optically pumped passive rubidium frequency standard," *Journal of Applied Physics*, vol. 53, no. 8, pp. 5387–5391, 1982.

[52] G. Missout and J. Vanier, "Pressure and temperature coefficients of the more commonly used buffer gases in rubidium vapor frequency standards," *IEEE Transactions on Instrumentation & Measurement*, vol. 24, no. 2, pp. 180–184, 2007.

[53] G. Iyanu, H. Wang, and J. Camparo, "Pressure sensitivity of the vapor-cell atomic clock," *IEEE Transactions on Ultrasonics Ferroelectrics & Frequency Control*, vol. 56, no. 6, pp. 1139–1144, 2009.

[54] D. Daoan, *Zhenkong Sheji Shouce*, National Defense Industry Press, 2004, (in Chinese).

[55] F. Yan, L. Detian, S. Ma, M. R. Guo, and H. Shen, "The inlet system of standard gas," *Vacuum and Cryogenics*, vol. 1, pp. 41–47, 2002, (in Chinese).

[56] M. Guo, L. Detian, F. Yan, and L. Zhao, "Performance study on reference gas intake system," *Vacuum*, vol. 41, 2004(in Chinese).

[57] K. Jousten, *Handbook of vacuum technology*, Wiley-VCH Verlag, 2008.

[58] C. Reber, *Upper Atmosphere Composition Data from Explorer XVII*, NASA, NTRS, 1964.

[59] P. T. Palmer and T. F. Limero, "Mass spectrometry in the U.S. space program: past, present, and future," *Journal of the American Society for Mass Spectrometry*, vol. 12, no. 6, pp. 656–675, 2001.

[60] E. R. Badman and R. Graham Cooks, "Miniature mass analyzers," *Journal of Mass Spectrometry*, vol. 35, no. 6, pp. 659–671, 2000.

[61] D. T. Snyder, C. J. Pulliam, Z. Ouyang, and R. G. Cooks, "Miniature and fieldable mass spectrometers: recent advances," *Analytical Chemistry*, vol. 88, no. 1, pp. 2–29, 2016.

[62] R. R. Syms, "Advances in microfabricated mass spectrometers," *Analytical and Bioanalytical Chemistry*, vol. 393, no. 2, pp. 427–429, 2009.

[63] G. L. Glish and R. W. Vachet, "The basics of mass spectrometry in the twenty-first century," *Nature Reviews Drug Discovery*, vol. 2, no. 2, pp. 140–150, 2003.

[64] H. D. Garcia, T. Limero, and J. T. James, "Setting spacecraft maximum allowable concentrations for 1 hour or 24 hour contingency exposures to airborne chemicals," in *International Conference on Evolvable Systems*, Seattle, WA, 1992.

[65] J. T. James, T. F. Limero, H. J. Leano, J. F. Boyd, and P. A. Covington, "Volatile organic contaminants found in the habitable environment of the space shuttle: STS-26 to STS-55," *Aviation, Space, and Environmental Medicine*, vol. 65, no. 9, pp. 851–857, 1994.

[66] J. F. Todd, S. J. Barber, I. P. Wright et al., "Ion trap mass spectrometry on a comet nucleus: the Ptolemy instrument and the Rosetta space mission," *Journal of Mass Spectrometry*, vol. 42, no. 1, pp. 1–10, 2007.

[67] C. Freissinet, A. Buch, R. Sternberg et al., "Search for evidence of life in space: analysis of enantiomeric organic molecules by N,N-dimethylformamide dimethylacetal derivative dependant gas chromatography-mass spectrometry," *Journal of Chromatography A*, vol. 1217, no. 5, pp. 731–740, 2010.

[68] R. Zhengyi, G. Meiru, C. Yongjun et al., "Design of a compact time-of-flight mass spectrometer for space application," *Journal of the American Society for Mass Spectrometry*, vol. 31, no. 2, pp. 434–440, 2020.

[69] Z. Ren, M. Guo, Y. Cheng et al., "Simulated and developed an electron impact ionization source for space miniature time-of-flight mass spectrometer," *Vacuum*, vol. 174, 2020.

[70] M. Guo, Z. Ren, Y. Cheng et al., "A new high precision, broad range gas micro-flow calibration apparatus," *Vacuum*, vol. 164, pp. 428–435, 2019.

[71] L. Gang, L. Detian, C. Yongjun et al., "Effect of voltage instability on motion characteristics of ions in ion trap," *Journal of Chinese Mass Spectrometry Society*, vol. 39, 2018(in Chinese).

[72] G. Li, D. Li, Y. Cheng et al., "Development of a low power miniature linear ion trap mass spectrometer with extended mass range," *Review of Scientific Instruments*, vol. 88, no. 12, p. 123108, 2017.

[73] G. Li, D. Li, Y. Cheng et al., "Improving the sensitivity of miniature linear ion trap mass spectrometer by a DC voltage applied on the eject electrodes," *European Journal of Mass Spectrometry*, vol. 24, no. 4, pp. 322–329, 2018.

[74] D. Li, M. Guo, Y. Xiao, Y. Zhao, and L. Wang, "Development of a miniature magnetic sector mass spectrometer," *Vacuum*, vol. 85, no. 12, pp. 1170–1173, 2011.

[75] D. Meng, C. Yongjun, S. Wenjun et al., "Newly developed compact magnetic sector mass spectrometer," *Measurement Science and Technology*, vol. 28, no. 12, article 125901, 2017.

[76] M. Guo, D. Li, Y. Cheng et al., "Performance evaluation of a miniature magnetic sector mass spectrometer onboard a satellite in space," *European Journal of Mass Spectrometry*, vol. 24, no. 2, pp. 206–213, 2018.

[77] J. HOFFMAN, R. CHANEY, H. HAMMACK et al., "Phoenix mars mission-the thermal evolved gas analyzer," *Journal of the American Society for Mass Spectrometry*, vol. 19, no. 10, pp. 1377–1383, 2008.

[78] L. J. Leger, S. L. Koontz, J. Visentine, and D. Hunton, "An overview of the evaluation of oxygen interaction with materials-third phase (Eoim-III) experiment: space shuttle mission 46. LDEF: 69 months in space," in *Third Post-Retrieval Symposium*, NASA Johnson Space Center, Houston, USA, 1995.

[79] J. A. Basford, M. D. Boeckmann, R. E. Ellefson et al., "Recommended practice for the calibration of mass spectrometers," *Journal of Vacuum Science and Technology*, vol. 11, no. 3, pp. A22–A40, 1993.

[80] L. Detian, L. Zhenghai, F. Yan et al., "Calibration system of partial pressure mass spectrometer," *Chinese Journal of Vacuum Science & Technology*, vol. 3, pp. 237–241, 2001, (in Chinese).

[81] D. Meng, S. Wenjun, W. Chengyao et al., "A UHV standard with option to be used as partial pressure standard," *Metrologia*, vol. 57, no. 2, article 025017, 2020.

[82] AIAA, "Status of the dawn ion propulsion system," in *AIAA/ASME/SAE/ASEE Joint Propulsion Conference & Exhibit*, Fort Lauderdale, Florida, 2004.

[83] N. Sillon and R. Baptist, "Micromachined mass spectrometer," *Sensors and Actuators B-Chemical*, vol. 83, no. 1-3, pp. 129–137, 2002.

[84] I. P. Wright, S. J. Barber, G. Morgan et al., "Ptolemy–an instrument to measure stable isotopic ratios of key volatiles on a cometary nucleus," *Space Science Reviews*, vol. 128, no. 1-4, pp. 363–381, 2007.

[85] D. Li, Y. Wang, Y. Cheng et al., "An overview of ionization gauges with carbon nanotube cathodes," *Journal of Physics D*, vol. 48, no. 47, 2015.

[86] H. Zhang, D. Li, P. Wurz et al., "Performance of a low energy ion source with carbon nanotube electron emitters under the influence of various operating gases," *Nanomaterials*, vol. 10, no. 2, p. 354, 2020.

[87] M. J. Milton, R. Davis, N. Fletcher et al., "Towards a new SI: a review of progress made since 2011," *Metrologia*, vol. 51, no. 3, pp. R21–R30, 2014.

[88] P. Szwemin, "How to characterize gas in high vacuum?," *Vacuum*, vol. 82, no. 2, pp. 174–177, 2007.

[89] K. Jousten, J. H. Hendricks, D. S. Barker et al., "Perspectives for a new realization of the Pascal by optical methods," *Metrologia*, vol. 54, no. 6, pp. S146–S161, 2017.

[90] L. Detian, C. Yongjun, and X. Zhenhua, "Development of quantum vacuum standard," *Journal of Astronautic Metrology and Measurement*, vol. 38, no. 3, pp. 1–15, 2018.

[91] X. Zhenhua, L. Detian, C. Yongjun et al., "Recent advances of vacuum metrology techniques and applications with optical methods," *Vacuum and Cryogenics*, vol. 22, no. 6, pp. 311–318, 2016.

[92] L. Yi, L. Detian, and W. Duoshu, "Research progress of cold atom quantum-based vacuum metrology," *Vacuum and Cryogenics*, vol. 25, no. 3, 2019.